Initial stages of growth and the influence of temperature during chemical vapor deposition of sp(2)-BN films

Mikhail Chubarov, Henrik Pedersen, Hans Högberg, Anne Henry and Zsolt Czigany

Original Publication:

Mikhail Chubarov, Henrik Pedersen, Hans Högberg, Anne Henry and Zsolt Czigany, Initial stages of growth and the influence of temperature during chemical vapor deposition of sp(2)-BN films, 2015, Journal of Vacuum Science & Technology. A. Vacuum, Surfaces, and Films, (33), 6, 061520.
http://dx.doi.org/10.1116/1.4935155

The initial stages of growth and the influence of temperature during chemical vapor deposition of sp^2-BN films

Running title: The initial stages of sp^2-BN films growth

Running Authors: Chubarov et al.

Mikhail Chubarov, Henrik Pedersen, Hans Högberg and Anne Henry[a)]

Linköping University, Department of Physics, Chemistry and Biology, SE-581 83 Linköping, Sweden

Zsolt Czigány

Institute of Technical Physics and Materials Science, Centre for Energy Research of Hungarian Academy of Sciences, Konkoly-Thege Miklós út 29-33, H-1121, Budapest, Hungary

[a)] Electronic mail: anne.henry@liu.se

Knowledge of the structural evolution of thin films, starting by the initial stages of growth is important to control the quality and properties of the film. We present a study on the initial stages of growth and the temperature influence on the structural evolution of sp^2 hybridized boron nitride (BN) thin films during chemical vapor deposition (CVD) with triethyl boron and ammonia as precursors. Nucleation of hexagonal BN (h-BN) occurs at 1200 °C on α-Al_2O_3 with an AlN buffer layer (AlN/α-Al_2O_3). At 1500 °C, h-BN grows with a layer-by-layer growth mode on AlN/ α-Al_2O_3 up to ~ 4 nm after which the film structure changes to rhombohedral BN (r-BN). Then r-BN growth proceeds with a mixed layer-by-layer and island growth mode. h-BN does not grow on 6H-SiC substrates; instead r-BN nucleates and grows directly with a mixed layer-by-layer and island growth mode. These differences may be caused by differences in substrate surface

temperature due to different thermal conductivities of the substrate materials. These results add to the understanding of the growth process of sp^2-BN employing CVD.

I. INTRODUCTION

Growth of thin film materials with well-defined mechanical, optical, and electrical properties is vital for many application areas in today's society. However, the aforementioned properties are highly dependent on for instance: the composition, the microstructure including the surface structure, the level of stress and grain size. For many applications there is a need to control all aspects of the thin film growth process, i.e. the initial formation of the nuclei on the substrate, their coalescence to form a continuous layer and finally the continued growth on this first layer to form a film of desired thickness. For the semiconductor materials AlN and GaN the growth mechanisms on both α-Al_2O_3 and SiC substrates are well investigated, allowing for high quality films to be deposited reproducibly. On α-Al_2O_3 a buffer layer is needed for deposition of high quality material. This layer usually is a GaN or an AlN layer grown at low temperature[1] and where layer-by-layer growth mode is observed after coalescence of the nucleation islands[2, 3]. The critical thickness for GaN growth on α-Al_2O_3 with an AlN buffer layer before the onset for dislocations due to lattice mismatch has been experimentally determined to 29 Å. This is in good agreement with the calculated value of 31.5 Å, using the equation derived by Fischer *et al*[4, 5]. On SiC substrates a similar behaviour to that of GaN on α-Al_2O_3 is observed for growth of GaN, while AlN solely proceeds in a layer-by-layer growth mode[6].

The literature on nucleation and growth of BN is sparse – especially for the sp^2-hybridised phases like hexagonal BN (h-BN) and rhombohedral BN (r-BN). Studies on the growth of sp^2-BN by chemical vapour deposition (CVD) on different substrates (Si, SiO_2/Si, quartz, α-Al_2O_3, SiC, Ni, Ru, Cu) and employing different boron ($B(C_2H_5)_3$, B_2H_6, BCl_3, BH_3-NH_3, $B_3N_3H_6$) and nitrogen (NH_3, N-plasma) precursors can be found in the literature[7-15]. The growth of sp^2-BN on metallic substrates is stimulated by the catalytic activity of the substrates usually employed (Ni, Ru, Cu, Pt) and is conducted at low growth temperature (ca. 1000 °C) but is limited to the growth of only a few basal planes of sp^2-BN before the catalytic metal surface is covered by BN[16-19]. The surface morphology of such films provides insights into the initial stages of thin film growth. In most cases formation of triangular-shaped islands on the substrate occurs leading to the conclusion that island growth mode is obtained[20-22]. Sutter *et al*[23] reported uniform coverage of the substrate with a few layers of sp^2-BN basal planes (up to 5) that suggests layer-by-layer growth mode, using growth by reactive magnetron sputtering. Most studies reporting on the growth of sp^2-BN on Si, α-Al_2O_3 and SiC substrates focus on the determination of the properties and quality of the deposited films while information on the initial stages of the growth is still lacking[8, 9, 14].

For CVD of sp^2-BN, an AlN buffer layer supports the growth of r-BN on α-Al_2O_3 substrates while no buffer layer was necessary to deposit r-BN on c-axis oriented SiC[24, 25]. Recently, we observed growth of h-BN on AlN buffer layer to a thickness of ~ 4 nm with a following transition to r-BN growth while polytype pure r-BN was observed on SiC substrates[26]. In the present study, we report on the nucleation and early stages of sp^2-BN growth on α-Al_2O_3 and SiC substrates for polytype and morphology control of sp^2-

BN films deposited by CVD. The formation of crystalline forms of sp^2-BN was investigated in the temperature range between 1200 °C and 1700 °C, to determine the growth conditions that favor the formation of r- or h-BN.

II. EXPERIMENTAL

To investigate the initial stages of growth for sp^2-BN thin films on α-Al_2O_3 with an AlN buffer layer (AlN/α-Al_2O_3) and on-axis (0001) 6H-SiC substrates we employed hot wall chemical vapour deposition (CVD) at a temperature of 1500 ^oC for 1, 5, 10, and 20 min of growth. A number of deposition experiments were carried out on both substrates at 1200 ^oC and on (0001) 6H-SiC at 1600 ^oC and 1700 ^oC. Triethylboron ($B(C_2H_5)_3$, TEB) and ammonia (NH_3) diluted in hydrogen (H_2) gas were the boron and nitrogen precursors, respectively. The TEB vapour was delivered into the reaction cell as carried by hydrogen gas that was bubbled through a stainless steel bubbler with the TEB liquid held at a constant pressure of 600 mbar and a constant temperature of 0 °C. This resulted in a TEB vapour pressure in the bubbler of ~20 mbar and with a TEB concentration in the total gas mixture of 135 ppm. The gaseous ammonia was fed to the reaction cell from a gas bottle. The flow was adjusted to obtain a nitrogen to boron ratio (N/B) of 643 at a growth temperature of 1500 °C and a ratio of 750 at a growth temperature of 1200 °C. In addition, silane (SiH_4) diluted in hydrogen to a concentration of 2000 ppm was added to the gas mixture to a total SiH_4 concentration of 5 ppm at 1500 ^oC and 1.2 ppm at 1200 ^oC following our previous results on the effect of silicon during growth of sp^2-BN thin films[27]. All depositions were conducted at a constant pressure of 70 mbar as controlled by a throttle valve installed before the process pump. The substrates were cleaned following the RCA procedure that includes removal of

organic contaminants by water solution of ammonia and hydrogen peroxide followed by removal of inorganic contaminants by water solution of hydrochloric acid and hydrogen peroxide[28]. Prior to the thin film deposition both type of substrates were *in situ* pre-treated, where an AlN buffer layer was formed on α-Al_2O_3 by nitridation at the applied growth temperature using ammonia at a total concentration 10 % in hydrogen during 10 minutes[24] or by the introduction of silane into the reactor at the temperature of 950 °C in order to improve the 6H-SiC substrate surface morphology[29].

The characterisation of the h-BN and r-BN structures is complicated as they show the same in-plane lattice constants (2.504 Å) and the same spacing between the basal planes (ca. 3.333 Å). When the film is grown epitaxially along the c-axis, h-BN and r-BN are difficult to distinguish by X-ray diffraction (XRD) in the Bragg-Brentano geometry (θ-2θ scan) or by transmission electron microscopy (TEM). However, it is possible to distinguish between them by observing the stacking sequence of the basal planes in atomic resolution TEM or by performing XRD measurements of diffraction peaks characteristic of the h-BN and r-BN phases. As a consequence, there are reports showing the formation of h-BN and r-BN when different growth conditions are employed[23, 30]. In addition, to these two crystalline forms of sp^2-BN, two less ordered forms exist: turbostratic (t-) and amorphous (a-) BN. The lack of the order between basal planes is characteristic for t-BN, which means that the basal planes are randomly rotated with respect to each other and do not have strictly defined spacing between them. This results in a slightly larger spacing between the basal planes compared to r- and h-BN, and where t-BN exhibits low intensity broad peaks in X-ray diffraction that is shifted to lower 2θ angles. In our previous work, we showed that the theoretically possible stackings of

sp^2-BN layers predicted by N. Ooi *et al*[31] are similar in X-ray diffraction to h-BN and should not be confused with r-BN[26].

XRD was used to determinate the structural properties of the deposited films. XRD measurements were performed by employing PANalytical EMPYREAN MRD X-Ray diffractometer equipped with a Cu-anode X-Ray tube and 5-axis (x-y-z-χ-φ) sample stage. For the determination of the crystalline structure of the thin films, Glancing Incidence XRD (GI-XRD) and investigation of asymmetric planes were conducted. GI-XRD allows for extracting information from the in-plane ordering of the film since the X-ray scattering vector is close to the sample surface plane (angles slightly higher than the critical angle for the material). Such geometry increases the sampling volume of the material. For these measurements capillary optics on the incident beam side and parallel plate collimator on the detector side were used. The Cu K_β line was removed by a Ni filter.

The stacking sequence and microstructure was assessed by electron microscopy from a JEOL 3010 instrument operated at an acceleration voltage of 300 kV and with 1.7Å point resolution. The sample was prepared in the way that it was cut along the $[1\bar{1}00]$ direction perpendicular to the (0001) plane of the h-BN as discussed in our previous work[26]. Such preparation allows the stacking sequence of the basal planes to be determined and the atomic resolution in TEM makes it possible to distinguish between r-BN and h-BN. Further, the TEM sample was prepared to a typical dimension of 1.8 x 0.5 x 0.5 mm^3 and were mounted and glued on a Ti grid[32] followed by mechanical thinning, polishing, and dimpling to a thickness of ~ 20 μm in the middle. Thinning to electron transparency was achieved by ion beam milling with 10 keV Ar^+ ions at an incidence

angle of 4° with respect to the surface. To minimize surface amorphization in the final period of the milling process, the ion energy was decreased gradually to 250 eV.

To study the formation of B-N bonds at the initial stages of growth we applied X-ray photoelectron spectroscopy (XPS) in a MICROLAB 310-F equipped with twin anode X-ray tube and using only the Al K_α line at generator settings of 15 kV and 20 mA and 5 x 2 mm^2 area of the sample being analysed. A spherical sector analyser and 5 channels detector were used to determine the energy of the photoelectrons emitted from the sample. The energy scale was calibrated from electrons emitted from the Fermi level that should have 0 eV binding energy in XPS.

Scanning electron microscopy (SEM) with a Leo 1550 instrument equipped with a field-emission gun was used to study the surface morphology of the deposited films. For the determination of 2D versus 3D growth, we used the observation by Sutter *et al*.[33] that the contrast in SEM when sp^2-BN is under investigation is directly related to the thickness of the BN layer. To reduce the charging effect due to the dielectric nature of the sp^2-BN especially on the insulating α-Al_2O_3 substrate an acceleration voltage of 5 kV was applied to the field emission gun.

III. RESULTS AND DISCUSSION

A. Nucleation and structure evolution

The early stages of sp^2-BN thin film growth were investigated on AlN/α-Al_2O_3. As can be seen from Figure 1 a-c, formation of triangular-shaped islands with a typical lateral size of ~ 500 nm is discernible on the surface after 20 minutes of growth (Figure 1c). The islands were evenly distributed on the surface, suggesting a layer-by-

layer growth of sp^2-BN for a limited thickness (growth time of 5 min <t< 20 min) followed by a transition to island or mixed layer-by-layer with island growth mode (t> 20 min). The hexagonal islands seen in Figure 1a and b are associated with the underlying AlN buffer layer and such islands were also observed on the surface of the α-Al_2O_3 following nitridation (Figure 2).

On (0001) 6H-SiC, the formation of triangular-shaped islands is seen after 5 minutes of growth (Figure 3 a-c), which is similar to that previously observed for BN growth on metallic substrates[20-22]. TEM shows the formation of a continuous layer of sp^2-BN on the SiC substrate (Supplementary figure 1)[34]. This continuous layer has not been observed on metallic substrates. Such growth behavior on the SiC substrate suggests layer-by-layer growth of sp^2-BN to a limited thickness (growth time t< 5 min) followed by a transition to island growth mode, i.e. the characteristic of mixed layer-by-layer and island growth modes. When studying SEM images obtained from sp^2-BN films deposited for 20 minutes, the surface of the film on SiC substrate appears to be covered by triangular-shaped islands with a density of ~ 4.4 μm^{-2} (Figure 3c). This can be compared to the well separated triangular islands visible on the AlN/α-Al_2O_3 with a density of ~ 1.7 μm^{-2} (Figure 1c). Thus sp^2-BN grows with a mixed layer-by-layer and island growth modes on both substrates while a transition to island growth mode occurs at a lower film thickness on 6H-SiC compared to AlN/α-Al_2O_3.

XPS measurements on the layers deposited for 1 minute on both substrates show the B 1s peak positioned at binding energies of around 189.5 eV, see (Figure 4). This value is close to the reported value for B-N bonding with binding energies in the range 189.9 to 190.7 eV[35-37], which support the formation of BN. The minor peak shifts in

Figure 4 is likely an effect of the non-conducting sapphire and semiconducting SiC substrates, leading to charging effect of the sample and shift of the Fermi level.

From the TEM micrograph in Figure 5 it can be seen that the atomic pairs of sp^2-BN deposited on AlN/α-Al_2O_3 are positioned directly on top of each other. This shows h-BN formation on AlN/α-Al_2O_3[26]. The film presented in Figure 5 was deposited for 10 minutes at 1500 °C with N/B=643 and pressure of 70 mbar and with 10 basal planes visible, which suggests a growth rate of 0.33 nm per minute (one basal plane per minute). This growth rate is more than 10 times lower compared to the growth rate determined for the thick (200 nm) films being 4 nm/min[26, 27]. A slow initial nucleation step that is followed by an increasing growth rate is often encountered in growth of thin film materials by CVD, e.g. diamond[38, 39] and SiC[40]. In our previous work, a transition from h-BN to r-BN growth on AlN/α-Al_2O_3 occurred after approximately 13 basal planes of h-BN[26] corresponding to a thickness of 43 Å. The transition of the growth from h-BN to r-BN on AlN/α-Al_2O_3 may be a consequence of stress relaxation induced by the lattice mismatch. Furthermore, the critical thickness for sp^2-BN growth on AlN by the Fischer equation[5] is 3 nm, which is in a good agreement with the experimentally observed h-BN thickness of ~4 nm[26]. Similar to our previous work[26], we used GI-XRD measurements to support the formation of h-BN by observing the peak from the $\{10\bar{1}0\}$ planes of h-BN and the peaks associated to the $\{11\bar{2}0\}$ planes of α-Al_2O_3 and $\{10\bar{1}0\}$ planes of AlN (not shown). In addition, the $10\bar{1}0$ peaks of h-BN were found confined and 60° separated in a ϕ scan suggesting epitaxial growth. This finding together with the observation that the basal planes of h-BN are parallel to the surface in the TEM micrograph leads to the conclusion that the h-BN film is grown epitaxially on the AlN/α-Al_2O_3 with epitaxial

relation $(11\bar{2}0)\ \alpha\text{-}Al_2O_3 \| (10\bar{1}0)AlN \| (10\bar{1}0)$h-BN and $(0001)\ \alpha\text{-}Al_2O_3 \| (0001)AlN \| (0001)$h-BN. This agrees with our previous results[24, 26]. Thus, it is possible to deposit phase pure epitaxial h-BN layer up to the thickness of about ~ 4 nm in a controlled way. The epitaxial growth determined by XRD suggests that the amorphous region at the interface visible in Figure 5 is an effect of the sample preparation.

B. Temperature effect on crystal evolution

To investigate the influence of temperature, we successfully grew h-BN on α-$AlN/\alpha\text{-}Al_2O_3$ at 1200 ^oC, by adjusting the N/B ratio and the SiH_4 content to 750 and 1.2 ppm, respectively. This growth conditions were achieved by gradually adjusting N/B ratio and SiH_4 flow where initial values were 640 and 0 respectively. The higher concentration of ammonia needed at lower temperature is an effect of a lower concentration of active species produced from ammonia molecule at lower temperatures [41]. The lower concentration of silane needed in the gas mixture at lower temperature can be attributed to a lower Si desorption rate from a less hot surface. The position of the h-BN 0002/ r-BN 0003 XRD peak for the samples deposited at 1200 °C is 26.65°±0.02° in 2θ, which differs from the typically observed value for samples deposited at 1500 °C of 26.74°. This peak shift towards the reference value for t-BN (26.3°)[42], where lower 2θ value implies that the ordering of the basal planes are somewhat lower in films deposited at 1200 °C[43]. To investigate the crystalline structure at the interface in layers deposited with short deposition time and a temperature of 1200 ^oC, we employed GI-XRD. Figure 6a shows θ-2θ scan where, similarly to high temperature grown layers, a peak associated

to the $\{10\bar{1}0\}$ planes of h-BN is observed along with the peaks from the $\{11\bar{2}0\}$ planes of α-Al_2O_3 and $\{10\bar{1}0\}$ planes of AlN and Figure 6b shows a ϕ scan of the $\{10\bar{1}0\}$ planes of h-BN which are separated by 60°. These results confirm the growth of h-BN on (0001) α-Al_2O_3 substrate with a AlN buffer layer. The ϕ scan also shows the epitaxial growth of h-BN at the temperature of 1200 °C. However, continuous growth of thicker film was difficult due to the formation of disordered, low density sp^2-BN (t-BN) that competes with crystalline material. The formation of such low density sp^2-BN films takes place also at higher temperature, but after a longer growth time (thicker film). The formation of t-BN is likely to be induced by a reduction of the surface temperature caused by the poor thermal conductivity of h- and r-BN in the c-axis direction. Another problem associated with the growth at low temperature is the enhanced memory effect of the reactor caused by lower desorption rate of adsorbed Si at lower temperature that complicates the control of the Si concentration in the gas phase. This makes deposition at 1200 °C hard to control and reproduce, and thus highly unstable as can be seen in the Supplementary figure 2 where the 0002/0003 peak position of h-BN/r-BN in XRD is plotted as a function of the Si concentration in the gas mixture[34].

For experiments on 6H-SiC, no peaks assigned to h-BN/r-BN (0002)/(0003) planes in XRD or $(10\bar{1}0)$ planes in GI-XRD in samples deposited below 1500 °C. As a matter of fact, there were no XRD peak visible corresponding to t-BN. However, peak characteristic of sp^2-BN at 1370 cm^{-1} was observed in Fourier transform infrared interferometry (Supplementary figure 3)[34]. From these observations we conclude that a-BN is formed.

For 6H-SiC substrates growth experiments were conducted at higher temperatures. At 1600 °C we found triangular-shaped islands characteristic for r-BN (Figure 7 a) but GI-XRD did not detect h-BN. A growth temperature of 1700°C was too high as the substrate was severely etched seen from the formation of etch craters (Figure 7 b).

From these observations as well as previously observed differences in triangular island densities we suggest that the growth of crystalline sp^2-BN requires higher temperature when 6H-SiC substrate is employed compared to when AlN/α-Al_2O_3 is utilized. This suggests a lower mobility of B and N adatoms on the surface of 6H-SiC, which prevents them from finding and occupying correct sites necessary for the formation of crystalline material. This leads to higher nucleation density and promotes formation of disordered sp^2-BN. Even at the growth temperature of 1200 °C h-BN formation is achieved on AlN/α-Al_2O_3 but r-BN only forms on 6H-SiC substrate at a higher growth temperatures ($T \geq 1500$ °C). We conclude that the growth of different sp^2-BN polytypes has a substrate promoted behavior, as discussed in our previous work[26].

IV. SUMMARY AND CONCLUSIONS

h-BN was deposited on (0001) AlN/(0001) α-Al_2O_3 at temperatures of 1200 °C and 1500 °C with an estimated growth rate of 0.33 nm/min. Following 12 minutes deposition time at 1500°C, a transition occurs from h-BN to r-BN, corresponding to a film thickness of 4 nm according to our recent HRTEM observation. This transition is supported from the formation of triangular islands characteristic of r-BN, which are observed in SEM after 20 minutes of growth. The h-BN growth evolves in a layer-by-layer growth mode, but for r-BN this is followed by a mixed layer-by-layer and island

growth mode. The change in sp^2-BN phase on AlN/α-Al_2O_3 substrate is suggested to be an effect of stress relaxation induced by the lattice mismatch. In contrast, on 6H-SiC substrates phase pure r-BN film grows directly with a mixed layer-by-layer and island growth mode.

The formation of different sp^2-BN polytypes is independent of the growth temperature, as h-BN forms on α-Al_2O_3 already at 1200 °C and growth transition from h-BN to r-BN occur after the critical film thickness at 1500 °C and r-BN grows directly on 6H-SiC at temperatures equal or higher than 1500 °C. From these observations the r-BN polytype is proposed to be thermodynamically favorable phase at our applied growth conditions.

ACKNOWLEDGMENTS

Sven G. Andersson is gratefully acknowledged for his help in maintaining the CVD equipment. This work was supported by the Swedish Research Council (VR: grant Nr. 621-2013-5585), Carl Tryggers Stiftelse (Nr. 12:175) and the CeNano program at Linköping University. HH acknowledges support from the Swedish Government Strategic Research Area in Materials Science on Functional Materials at Linköping University (Faculty Grant SFO-Mat-LiU Nr. 2009-00971). ZC acknowledges the support of Bolyai Janos research scholarship of Hungarian Academy of Sciences.

REFERNCES

1 S. Strite, H. Morkoc, J. Vac. Sci. Technol. B. **10**, 1237 (1992).

2 X. Sun, D. Li, Y. Chen, H. Song, H. Jiang, Z. Li, G. Miao, Z. Zhang, CrystEngComm **15**, 6066 (2013).

3 K. Hiramatsu, S. Itoh, H. Amano, I. Akasaki, J. Cryst. Growth **115**, 628 (1991).

4 C. Kim, I.K. Robinson, J. Myoung, K. Shim, M.C. Yoo, K. Kim, Appl. Phys. Lett. **69**, 2358 (1996).

5 A. Fisher, H. Kuhne, H. Richter, Phys, Rev. Lett. **73**, 2712 (1994).

6 R.F. Davis, R.D. Bremser, W.G. Perry, K.S. Ailey, J. Eur. Ceram. Soc. **17**, 1775 (1997).

7 M. C. Polo, M. B. el Mekki, J. L. Andujar, N. Mestres, J. Pascual, Diamond Relat. Mater. **6**, 1550 (1997).

8 M. Anutgan, T. Aliyeva Antugan, E. Ozkol, I. Atilgan, B. Katircioglu, J. of Non-Cryst. Solids **355**, 1622 (2009).

9 Y. Kobayashi, T. Akasaka, T. Makimoto, J. Cryst. Growth **310**, 5048 (2008).

10 R. Y. Tay, M. H. Griep, G. Mallick, S. H. Tsang, R. S. Singh, T. Tumlin, E. H. T. Teo, S. P. Karna, Nano Lett **14**, 839 (2014).

11 S. Le Gallet, G. Chollon, F. Rebillat, A. Guette, X. Bourrat, R. Naslain, M. Couzi, J. L. Bruneel, J. Eur. Ceram. Soc. **24**, 33 (2004).

12 R. Y. Tay, X. Wang, S. H. Tsang, G. C. Loh, R. S. Singh, H. Li, G. Mallick, E. H. T. Teo, J. Mater. Chem. C **2**, 1650 (2014).

13 M. T. Paffett, R. J. Simonson, P. Papin, R. T. Paine, Surf. Sci. **232**, 286 (1990).

14 R. Dahal, J. Li, S. Majety, B. N. Pantha, X. K. Cao, J. Y. Lin, H. X. Jiang, Appl. Phys. Lett. **98**, 211110 (2011).

15 R. Y. Tay, S. H. Tsang, M. Loeblein, W. L. Chow, G. C. Loh, J. W. Toh, S. L. Ang, E. H. T. Teo, Appl. Phys. Lett. **106**, 101901 (2015).

16 L. Song, L. Ci, H. Lu, P. B. Sorokin, C. Jin, J. Ni, A. G. Kvashnin, D. G. Kvashnin, J. Lou, B. I. Yakobson, P. M. Ajayan, Nano Lett. **10**, 3209 (2010).

17 P. Sutter, E. Sutter, APL Matter. **2**, 092502 (2014).

18 A. Hemmi, C. Bernard, C. Hun, S. Roth, M. Klockner, T. Kalin, M. Weinl, S. Gsell, M. Schreck, J. Osterwalder, T. Greber, Rev. Sci. Insrtum. **85**, 035101 (2014).

19 A. Gibb, N. Alem, A. Zettl, Phys. Status Solidi B **250**, 2727 (2013).

20 C. J. Kim, L. Brown, M. W. Graham, R. Hovden, R. W. Havener, P. L. McEuen, D. A. Muller, J. Park, Nano Lett. **13**, 5660 (2013).

21 S. M. Kim, A. Hsu, P. T. Araujo, Y. H. Lee, T. Palacios, M. Dresselhaus, J. C. Idrobo, K. K. Kim, J. Kong, Nano Lett. **13**, 933 (2013).

22 S. Joshi, D. Ecija, R. Koitz, M. Iannuzzi, A. P. Seitsonnen, J. Hutter, H. Sachdev, S. Vijayaraghavan, F. Bischoff, K. Seufert, J. V. Barth, W. Auwarter, Nano Lett. **12**, 5821 (2012).

23 P. Sutter, J. Lahiri, P. Zahl, B. Wang, E. Sutter. Nano Lett. 13, 276 (2013).

24 M. Chubarov, H. Pedersen, H. Högberg, V. Darakchieva, J. Jensen, P.O.Å. Persson, A. Henry. Phys. Status Solidi RRL **5**, 397 (2011).

25 M. Chubarov, H. Pedersen, H. Högberg, Zs. Czigany, A. Henry, CrystEngComm. **16**, 5430 (2014).

26 M. Chubarov, H. Pedersen, H. Högberg, Zs. Czigany, M. Garbrecht, A. Henry, Chem. Mater. **27**, 1640 (2015).

27 M. Chubarov, H. Pedersen, H. Högberg, A. Henry. CrystEngComm **15**, 455 (2013).

28 K. A. Reinhardt, W. Kern, *Handbook of silicon wafer cleaning technology* (William Andrew Inc. USA, 2008)

29 J. Hassan, J. P. Bergman, A. Henry, E. Janzen, J. Cryst. Growth **310**, 4430 (2008).

30 M. Chubarov, H. Pedersen, H. Högberg, J. Jensen, A. Henry. Cryst. Growth Des. **12**, 3215 (2012).

31 N. Ooi, A. Rairak, L. Lindsley, J. B. Adams, J. Phys.: Condens. Matter **18**, 97 (2006).

32 Á. Barna. Mater. Res. Soc. Symp. Proc. **254**, 3 (1992).

33 P. Sutter, E. Sutter, APL Matter. **2**, 092502 (2014).

34 See supplemental material at **[URL will be inserted by AIP]** for additional clarifying figures.

35 M. Antugan, T. Aliyeva-Antugan, E. Ozkol, I. Atilgan, B. Katircioglu, J. Non-Cryst. Solids **355**, 1622 (2009).

36 L. Song, L. Ci, H. Lu, P. B. Sorokin, C. Jin, J. Ni, A. G. Kvashnin, D. G. Kvashnin, J. Lou, B. I. Yakobson, P. M. Ajayan, Nano Lett. **10**, 3209 (2010).

37 Y. Shi, C. Hamsen, X. Jia, K. K. Kim, A. Reina, M. Hofmann, A. L. Hsu, K. Zhang, H. Li, Z.-Y. Juang, M. S. Dresselaus, L.-J. Li, J. Kong, Nano Lett. **10**, 4134 (2010).

38 J. Wei, J. M. Chang, Y. Tzeng. Thin Solid Films **212**, 91 (1992).

39 H. Sternschulte, M. Schreck, B. Stritzker. Diamond Rel. Mater **11**, 296 (2002).

40 A. Henry, L. Storasta, E. Janzén, Mater. Sci. Forum **433-436**, 153 (2003).

41 B. Beaumont, P. Gibart, J. P. Faurie, J. Cryst. Growth **156**, 140 (1995).

42 Joint Committee on Powder Diffraction Standards, JCPDS, Swarthmore, PA, pattern 34 – 0421; pattern 45 – 1171.

43 C. Schimpf, M. Motylenko, D. Rafaja, Mater. Charact. **86**, 190 (2013).

Figure captions:

FIG. 1. SEM images of films deposited on α-Al_2O_3 for (a) 1 minute, (b) 5 minutes and (c) 20 minutes where one of the islands is highlighted with a red triangle.

FIG. 2. SEM image of the AlN buffer layer formed on α-Al_2O_3 by nitridation at 1500 °C for 10 minutes with NH_3 concentration of 10 % in H_2 carrier gas and at a pressure of 70 mbar. The image shows the surface of the AlN buffer layer that allows concluding that islands observed in Figure 1a are related to the buffer layer and not to sp^2-BN. Insert shows 3.6 times magnified part of the surface.

FIG. 3. SEM images of films deposited on 6H-SiC for (a) 1 minute, (b) 5 minutes and (c) 20 minutes.

FIG. 4. XPS spectra of the B 1s peaks for films deposited for 1 minute on (a) 6H-SiC and (b) α-Al_2O_3.

FIG. 5. HRTEM micrograph of a film deposited for 10 minutes on AlN/α-Al_2O_3. Alignment of the atomic planes in the BN film suggests formation of pure h-BN. The amorphous region between the AlN and h-BN could be an effect of interface amorphization or film exfoliation.

FIG. 6. GI-XRD patterns showing (a) θ-2θ scan and (b) ϕ scan of the film deposited on AlN/α-Al_2O_3 at 1200 °C showing formation of epitaxial h-BN.

FIG. 7. SEM images of films deposited on 6H-SiC substrate at (a) 1600 °C and (b) 1700 °C. Triangular –shaped islands that are characteristic for r-BN are observed at both conditions while at the temperature of 1700 °C size and density of such triangles are lower than at growth temperature of 1600 °C. In the right image, due to low contrast of the triangles on the background white arrows are pointing on some of them.

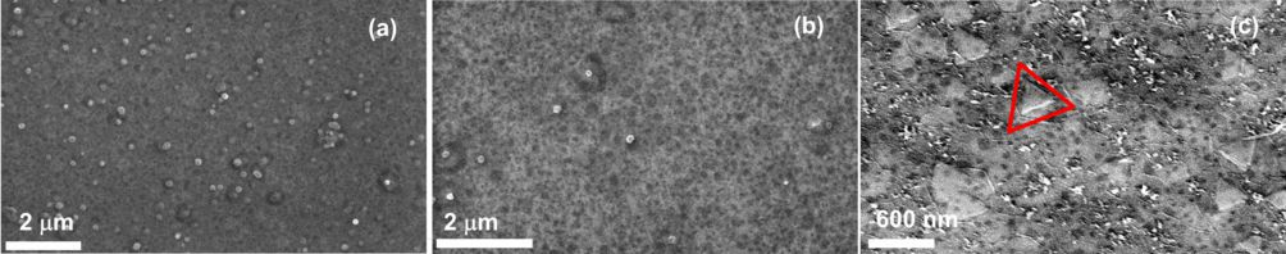
(a)
2 μm
(b)
2 μm
(c)
600 nm

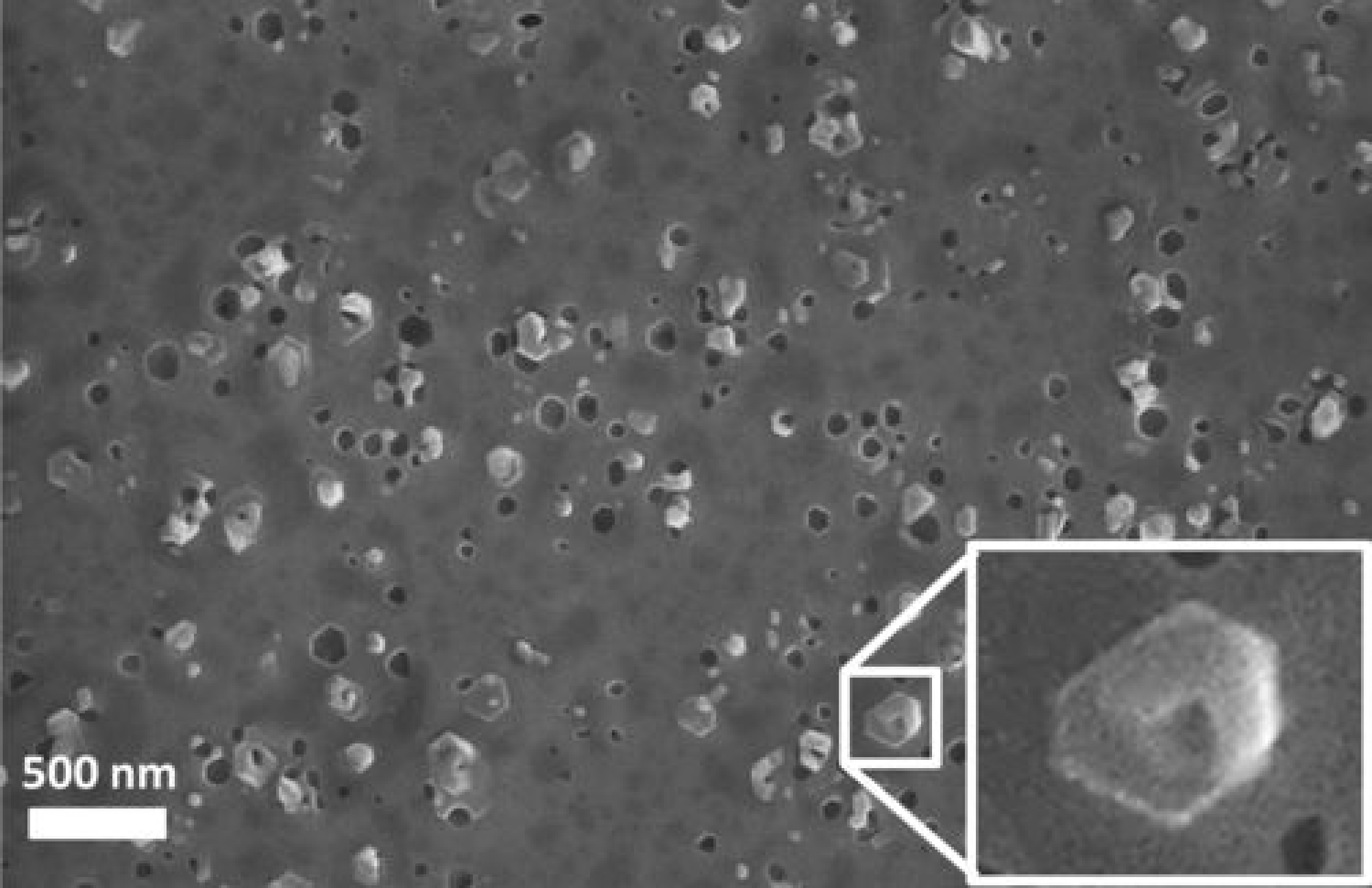
500 nm

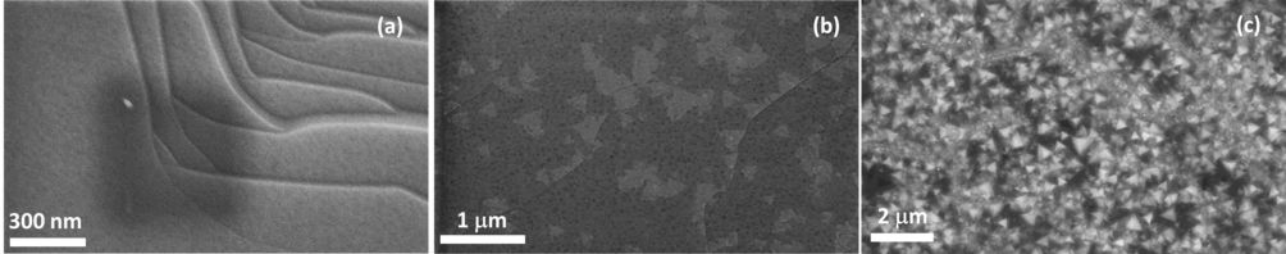
(a)
300 nm
(b)
1 μm
(c)
2 μm

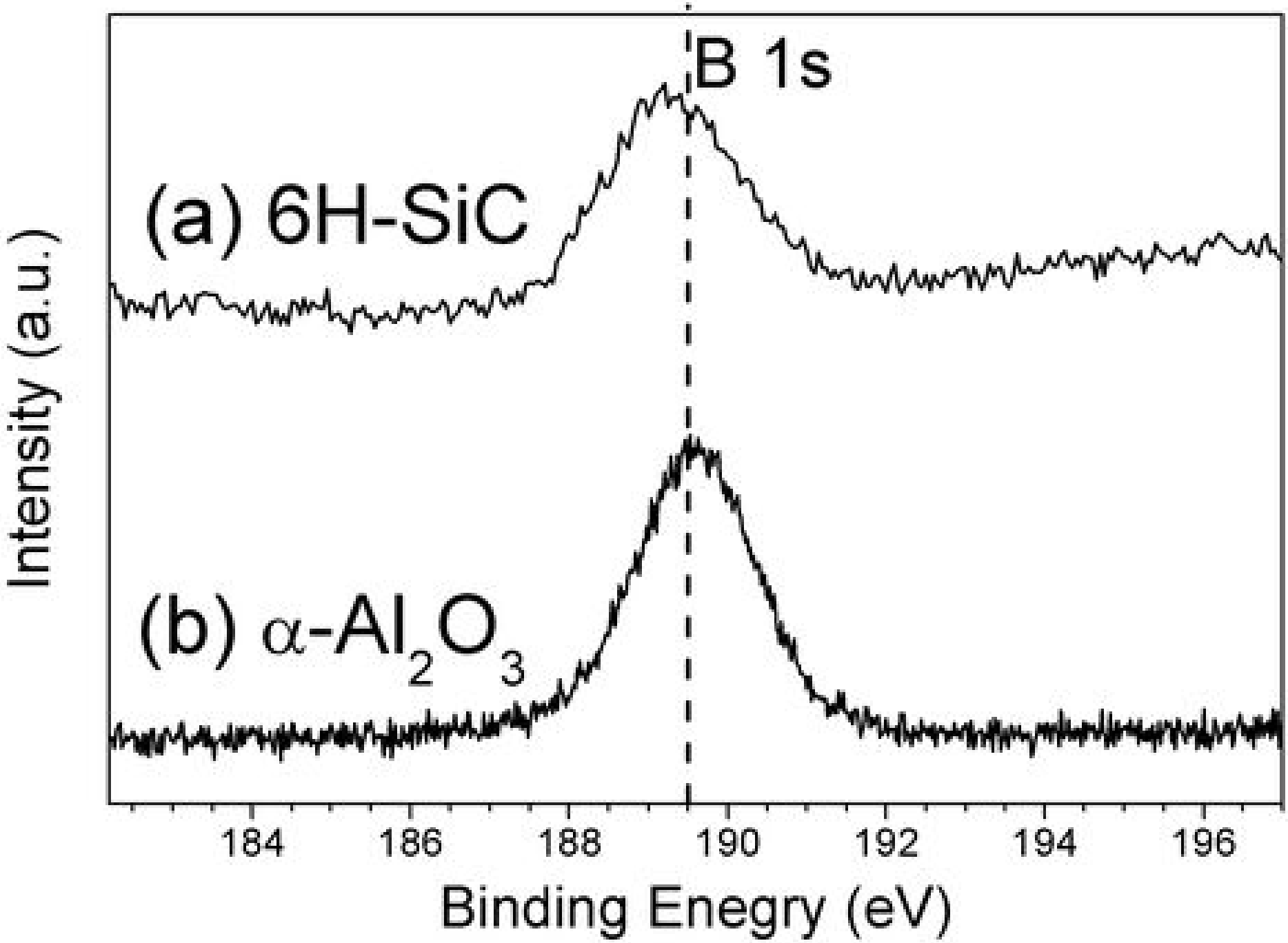
B 1s
(a) 6H-SiC
(b) α-Al2O3
Intensity (a.u.)
184
186
188
190
192
194
196
Binding Enegry (eV)

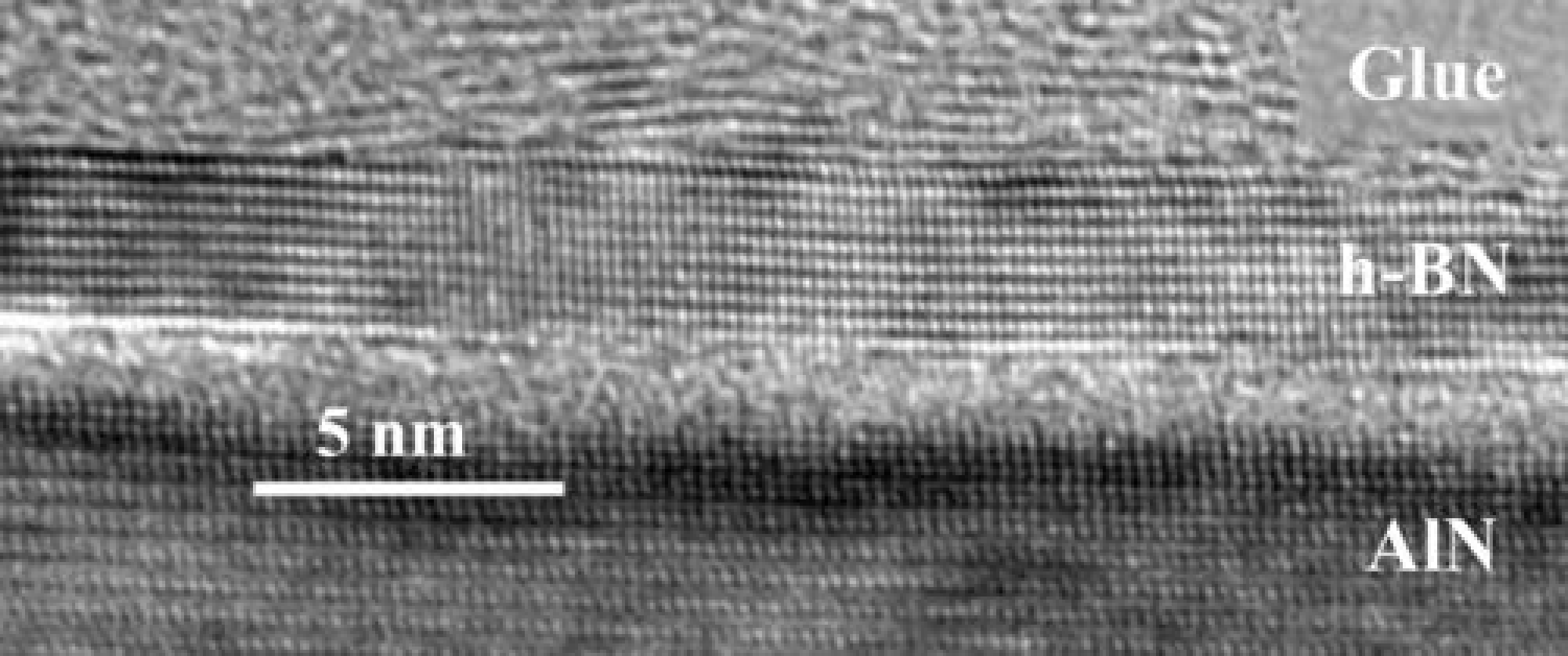
Glue
h-BN
5 nm
AlN

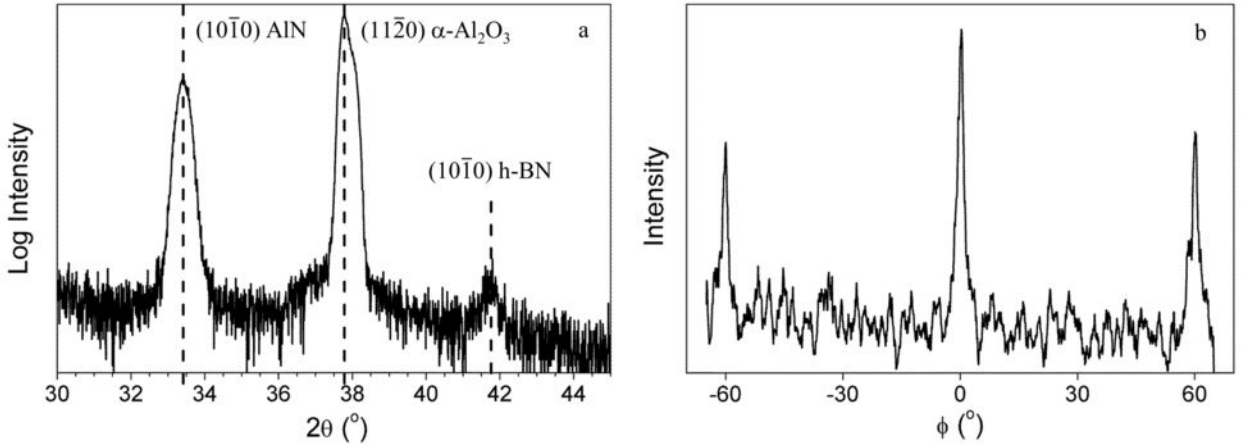
(10$\bar{1}$0) AlN
(11$\bar{2}$0) α-Al_2O_3
a
(10$\bar{1}$0) h-BN
Log Intensity
30
32
34
36
38
40
42
44
2θ (°)
b
Intensity
-60
-30
0
30
60
ϕ (°)

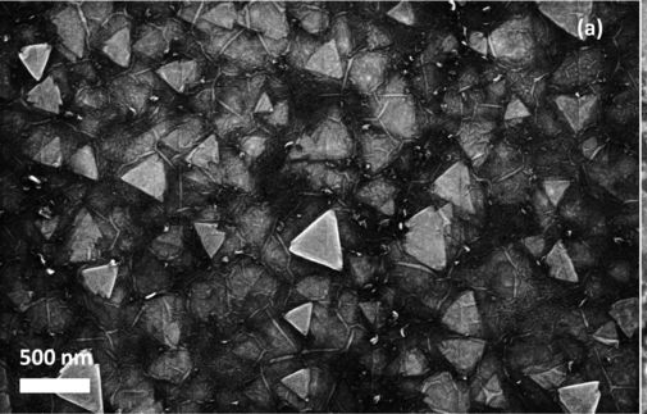
(a)
500 nm

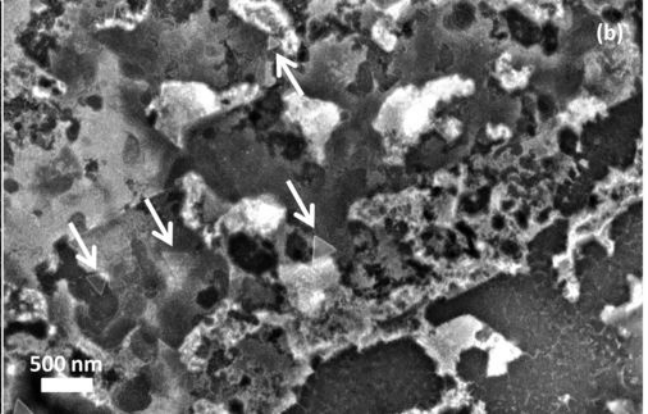
(b)
500 nm